Identification of a Chameleon-like pH-Sensitive Segment within the Colicin E1 Channel Domain That May Serve as the pH-Activated Trigger for Membrane Bilayer Association†

A. Rod Merrill,*,‡ Brian A. Steer,‡,§ Gerry A. Prentice,‡ Mike J. Weller,|| and Arthur G. Szabo||

Guelph-Waterloo Centre for Graduate Work in Chemistry, Department of Chemistry and Biochemistry, University of Guelph, Guelph, Ontario N1G 2W1, Canada, and Department of Chemistry and Biochemistry, University of Windsor, Windsor, Ontario N9B 3P4, Canada

Received January 30, 1997; Revised Manuscript Received April 9, 1997⊗

ABSTRACT: *In vitro,* the channel-forming domain of colicin E1 requires activation by acidic pH (<4.5) or detergents. The activation of this domain to its insertion-competent state results in an increased ability of the protein to dock onto and to form channels in artificial membranes. Fluorescence methods were used to characterize the conformational changes occurring in a channel-forming peptide of colicin E1 in solution with pH. The 178-residue thermolytic fragment of colicin E1 contains three Trp residues, W-424, W-460, and W-495. In order to study the structural and dynamic requirements for activation of the C-terminal domain of colicin E1, single-Trp-containing peptides were prepared by site-directed mutagenesis. All of the mutant peptides displayed *in vitro* channel activity and cellular cytotoxicity similar to the those of wild-type peptide. Two Trp residues, W-413 and W-424, exhibited pH-sensitive fluorescence parameters. Upon acidification (pH 6.0 → 3.5), the fluorescence quantum yield of W-413 and W-424 increased 50% and 80%, respectively, indicating a significant change in the local environment of the peptide segment containing these two Trp residues. The fluorescence decay of W-413 and W-424 was best fit by three fluorescence decay components, two of which were sensitive to pH. However, only small changes in spectral shape and position were observed for W-424 fluorescence, whereas there were larger changes in these fluorescence parameters for W-413. The quantum yields for the Trp residues in the seven other single-Trp mutant peptides and the wild-type peptide were distinct but only slightly affected by changes in pH. Time-resolved fluorescence measurements showed that W-460, -484, and -495 each had two fluorescence decay components with similar decay times, with one component dominating the fluorescence decay behavior. Furthermore, the individual fluorescence decay times for all the single-Trp peptides, except for W-413 and W-424, were insensitive to pH changes. At pH 3.5, the fluorescence of the wild-type peptide was fit by three decay time components, with the two longer decay times being quite different from the fluorescence decay times of the single-Trp mutant proteins (W-424, -460, and -495, the naturally occurring Trp residues). In contrast, at pH 6.0, the wild-type peptide showed double-exponential decay kinetics. Time-resolved fluorescence anisotropy decay measurements of the three single-Trp mutant proteins, containing a naturally occurring Trp residue, suggest that local segmental motion of the peptide as reported by each of the three tryptophans is highly restricted and largely insensitive to changes in pH. On the other hand, the anisotropy decay profiles of the wild-type protein were consistent with energy transfer occurring between Trp residues, likely between W-460 and W-495. These steady-state and time-resolved fluorescence results show that W-413 and W-424 report conformational changes which may be associated with the insertion-competent state and reside on the protein segment(s) which form the pH-activated trigger of the channel peptide.

Many protein toxins such as diphtheria toxin (*1*) and *Pseudomonas aeruginosa* exotoxin A (*2*) and protein-like toxins such as the bactericins, colicin A and E1, require low pH for *in vitro* activity (*3*, *4*). Considerable work has focused on the determination of the protein structural events that occur when these proteins are activated and on the role of low pH in the activation process. The colicin E1 channel domain is a helical bundle protein composed of 11 α-helices arranged in three layers (P. Elkins, personal communication). A hairpin of hydrophobic helices makes up the middle layer of the structure. Previously, it was demonstrated that the channel peptide of colicin E1 does not undergo a large "unfolding" upon activation to its insertion-competent state, but rather that this activation induced by low pH or detergent involves a more subtle conformational change (*5*). Subsequently, Schendel and Cramer (*6*) presented evidence that it is unlikely that a local lower pH at the membrane surface significantly facilitates formation of an unfolded intermediate. However, the aforementioned studies were all limited by their inability to obtain site-specific data on the channel peptide as a function of pH.

† Supported by the Natural Sciences and Engineering Research Council of Canada (A.R.M. and A.G.S.). B.A.S. was the recipient of a NSERC predoctoral scholarship.

* Author to whom correspondence should be addressed. Telephone: 519-824-4120 ext. 3806. Fax: 519-766-1499. E-mail: Merrill@chembio.uoguelph.ca.

‡ University of Guelph.

§ Present address: Department of Biology, 68-230, Massachusetts Institute of Technology, 77 Massachusetts Ave., Cambridge, MA 02139.

|| University of Windsor.

⊗ Abstract published in *Advance ACS Abstracts,* May, 15, 1997.

S0006-2960(97)00222-5 CCC: $14.00

Previously, site-specific information on protein structure was obtained through the use of a combination of site-directed mutagenesis techniques where Trp residues were introduced into different segments of the calcium-binding tumor protein oncomodulin, with fluorescence spectroscopic methods. This approach provided new insights into the influence of metal binding on the structure of the oncomodulin protein (*7*) and provided a useful approach to the study of protein solution structure and dynamics. Also, new insights into the structure and function of a number of other proteins, including a bacterial Trp repressor protein (*8*), phosphofructokinase from *Bacillus stearothermophilus* (*9*), the extracellular domain of human tissue factor (*10*), and a bovine protein tyrosyl phosphatase (*11*), have been obtained by site-specific time-resolved fluorescence analysis. In an effort to probe the events occurring upon low-pH activation of the thermolytic channel peptide of colicin E1, single-Trp-containing mutant proteins were prepared by site-directed mutagenesis so that the Trp residues can serve as intrinsic fluorescence probes of the conformational heterogeneity and local segmental flexibility of the channel peptide (*12*−*14*).

Earlier, a study of the degree of solvent exposure for 12 single-Trp channel peptides of colicin E1 was reported (*13*). None of the three naturally occurring Trp residues (W-495, -460, and -424) exhibited significant changes in the extent of solvent exposure upon low-pH activation. However, Trp residues located in the amino-terminal end of the channel peptide (W-355, -367, -393, -413, and -443) reported significant changes in the extent of solvent accessibility upon low-pH activation of the peptide. The unfolding of the amino- terminal end of the peptide upon low-pH activation was given further credence by the results of Steer and Merrill (*14*), who used fluorescence resonance energy transfer (FRET)[1] and determined the relative changes in FRET efficiency with detergent activation of various donor (Trp residues) and acceptor (AEDANS) pairs. These results, taken together, lead to the proposal of the "extension cord model" for colicin E1 channel peptide activation. This model features the core of the soluble protein being composed of the C-terminal one-third of the molecule, including a hydrophobic region of 35 amino acid residues, with the amino-terminal residues wrapped around the core in a coiled manner, which partially unravels upon low-pH activation. A subsequent study also involved the use of single-Trp mutant channel peptides to study the folding mechanism of the soluble colicin E1 channel peptide (*15*).

In the present study, the WT and nine single-Trp mutant peptides of the colicin E1 thermolytic channel peptide were studied by fluorescence spectroscopic techniques. Both steady-state and time-resolved fluorescence analyses were conducted on the proteins to monitor site-specific events within the protein structure in response to low-pH activation. These experiments provide insight into the mechanism of pH activation of the colicin E1 channel peptide to its insertion-competent state.

[1] Abbreviations: AEDANS, 5-[[[(iodoacteyl)amino]ethyl]amino]naphthalene-1-sulfonic acid; DAS, decay-associated spectra; DMG, dimethyl glutarate; FRET, fluorescence resonance energy transfer; FWHM, full width at half-maximum; HPLC, high-performance liquid chromatography; λ_{em}max, fluorescence emission maximum; MES, 2-(*N*-morpholino)ethanesulfonic acid; NATA, *N*-acetyltryptophanamide; Q_F, fluorescence quantum yield; SDS−PAGE, sodium dodecyl sulfate−polyacrylamide gel electrophoresis; Trp^-, tryptophan-deficient peptide; WT, wild-type peptide.

MATERIALS AND METHODS

Preparation and Purification of the Colicin E1 and Carboxyl-Terminal Thermolytic Peptide. Colicin E1 was prepared and purified from JC411 or DM1187 cells harboring a colicin E1-encoding plasmid, pDMS630, as described previously (*5*, *16*). The preparation of the carboxyl-terminal thermolytic peptide of colicin E1 was accomplished as described earlier (*5*).

The single-Trp-containing channel peptides used in the fluorescence experiments were further purified by high-performance liquid chromatography (HPLC) using an ion-exchange column (Biorad MA7S cation-exchange, 50 × 7.8 mm). The starting buffer was 50 mM MES (Sigma Chemical Co., St. Louis, MO) at pH 6.0, and the channel peptide eluted between 150 and 200 mM NaCl. Overloading of an SDS−PAGE gel (*17*) with purified peptide revealed less than 1% contamination from protein impurities. Furthermore, the amino acid analysis of the single-Trp channel peptides was consistent with the known residue composition calculated from the protein sequence (*13*, *18*). In addition, the absorption spectra of the single-Trp mutants revealed that the protein preparations were devoid of any nonprotein contaminating chromophores.

Preparation of Single-Trp Mutants of Colicin E1. The preparation of colicin E1 mutants possessing a single Trp residue in the carboxyl-terminal fragment has been described (*12*, *13*) in which Phe residues were substituted for the two endogenous Trp residues. Also, a fourth colicin E1 mutant was prepared which was devoid of any Trp residue[2] in the channel domain. Subsequently, Trp residues were added to the channel peptide to prepare additional single-Trp mutant peptides by substituting for either Phe or Tyr residues. Each of the mutant whole colicin proteins was tested for cytotoxicity by a "spot test" on a bacterial lawn of sensitive *Escherichia coli* cells (strain B), and all were similar to the wild-type colicin (*13*). Also, *in vitro* measurements of colicin channel activity were performed as previously described (*12*, *14*) and confirmed that aromatic amino acid substitution in the carboxyl-terminal domain of colicin E1 did not affect normal channel function.

Spectroscopic Measurements. All samples of the proteins used in the spectroscopic measurements were buffered solutions (100 mM NaCl and 10 mM dimethyl glutarate) at pH 3.5 or 6.0, at a temperature of 20 °C unless otherwise stated. The concentration of the proteins was usually 60 μg/mL. Absorption spectra were measured on a either a Perkin-Elmer λ-6 or a Varian DMS 200 spectrometer, both computer-interfaced and equipped with thermostated reference and sample cell holders attached to a constant-temperature water bath.

Time-resolved fluorescence measurements were performed using the technique of time-correlated single-photon counting

[2] The notations W-424, W-460, and W-495 designate the Trp residue within the corresponding mutant colicin E1 channel peptide where the other Trp residues have been replaced by a Phe residue. W-404, -413, -431, -443, and -484 refer to the Trp residues within the corresponding mutant channel peptides of colicin E1 where the naturally occurring Trp residues (W-424, -460, and -495) have been replaced with Phe residues and a Trp residue has been substituted for a Phe. In the case of W-367, a Tyr residue has been replaced with a Trp. WT refers to the wild-type peptide which contains all of the three endogenous Trp residues.

with instrumentation and data analysis procedures described previously (*19*). The excitation source was a cavity-dumped dye laser synchronously pumped by an actively mode-locked argon ion laser (Spectra Physics) operating at 825 kHz with a pulse width of 15 ps. Fluorescence resulting from vertically polarized excitation at either 295, 300, or 305 nm was detected at right angles after passing through a polarizer set at 55° to the vertical and a JY H10 monochromator, with a 4 nm band-pass, on a Hamamatsu 1564U-01 microchannel plate photomultiplier. The channel width was either 21.6 or 10.8 ps, and the data were collected in 1024 channels of a Nucleus multichannel analyzer. The instrument response function determined from the Raman scatter water signal was typically 80 ps/channel. Each decay curve contained at least 5×10^5 to 1.5×10^6 total counts and required ca. 3 min of data collection time. The ratio of laser pulses to single photon events was 100:1 or greater. In all cases, a buffer blank was also measured under conditions identical to those of the sample and it was subtracted from the sample signal prior to data analysis. Appropriate weighting of the sample decay profile was used to account for this subtraction procedure.

The data were analyzed according to a model in which the fluorescence decayed as a sum of exponentials. The adequacy of the exponential decay fitting was judged by the inspection of the plots of weighted residuals and different statistical parameters (*20*). The fluorescence decay profiles taken at different emission wavelengths across the fluorescence spectrum were first analyzed individually. Since the data showed that the values of the decay times did not vary significantly across the fluorescence spectrum, they were then analyzed by global nonlinear least-squares iterative convolution methods (*21*, *22*). Decay-associated spectra (DAS), the fluorescence spectra associated with each individual decay component, were constructed from the fluorescence decay parameters obtained from the global analysis and the steady-state fluorescence spectra.

Fluorescence anisotropy decay measurements were performed with the time-correlated single-photon counting laser system. The excitation beam was vertically polarized. The fluorescence passed through a Glan Taylor calcite polarizer which was set at either 0 or 90° to the excitation polarization direction. The vertically and horizontally polarized fluorescence decay curves, I_{VV} and I_{VH}, respectively, were measured sequentially for identical periods of "live time" data accumulation. A solvent blank for each polarization direction was measured for the same period of time and subtracted from the corresponding polarized fluorescence decay profile. A correction factor, *G*, for the intensity sensitivity of the different polarization directions was determined by measuring the vertically and horizontally polarized fluorescence decay of a sample of azanaphthene in ethanol solution, each for the same "live time" accumulation. The counts in these latter decay curves were summed in all channels corresponding to times greater than 3 ns. The azanaphthene fluorescence was considered isotropic after that time. The ratio of these integrated values for azanaphthene, I_{VV}/I_{VH}, was the correction factor by which the horizontally polarized fluorescence decay curve of the sample was multiplied. The vertically and horizontally polarized decay curves were then analyzed simultaneously using global analysis techniques where

$$I_{VV}(t) = {}^1/_3\alpha_i \exp(-t/\tau_i)[1 + 2r(t)] \quad (1)$$

$$I_{VH}(t) = {}^1/_3\alpha_i \exp(-t/\tau_i)\,[1 - r(t)] \quad (2)$$

$$r(t) = (r_o - r_\infty)\exp(-t/\theta_j) + r_\infty \quad (3)$$

The terms α_i and τ_i are the pre-exponential value and the corresponding fluorescence decay time of the *i*th component, respectively. The terms r_o, r_∞, and θ_j correspond to the initial anisotropy, the anisotropy at $t = \infty$ (plateau value), and the rotational correlation time of the *j*th rotational component, respectively. The anisotropy decay curves $r(t)$ presented in the figures were derived from the expression

$$r(t) = [I_{VV}(t) - I_{VH}(t)G]/[I_{VV}(t) + 2I_{VH}(t)G] \quad (4)$$

Determination of Fluorescence Quantum Yields (Q_F). Steady-state fluorescence measurements were made with either a PTI spectrofluorimeter or a SLM 8000C spectrofluorimeter operating in the ratio mode, with unpolarized excitation and an emission polarizer (Glan-Taylor) oriented at 35° to the vertical to eliminate any effects of anisotropy on quantum yield or intensity measurements. The signal from the buffer blank was subtracted from the sample fluorescence, and the spectra were corrected for the wavelength dependence of the instrument response. Steady-state fluorescence anisotropy measurements were made using "T-format" detection with the excitation being vertically polarized. The "*G*" instrumental factor, I_{HV}/I_{HH}, was determined using horizontally polarized excitation. Each anisotropy value is the mean of three determinations, where each measurement was made for an integration time of 15 s. A solvent blank was subtracted from each intensity reading prior to the calculation of the anisotropy value. Fluorescence quantum yields (Q_F) for each of the proteins were measured at 20 °C, using *N*-acetyltryptophanamide (pH 7.0) as a standard as previously described (*23*). The excitation wavelength was either 295 or 300 nm (identical results were obtained with either), and the excitation and emission band-pass were both 2 nm. The absorbance of the samples at the excitation wavelength was typically less than 0.1. The values reported represent the mean of at least three determinations, but in some cases, ten measurements were required.

Molecular Modeling Experiments. Molecular modeling experiments on the 2.5 Å resolution X-ray structure of the colicin E1 channel peptide (coordinates kindly provided by P. Elkins) were performed on an IBM RISC System 6000 computer workstation using the Biosym Insight II software package.

RESULTS AND DISCUSSION

Location of Trp in the Various Single-Trp Channel Peptides. The primary sequence for the colicin E1 thermolytic channel peptide (MW of 19 700 Da; N terminus, I-345) is shown in Figure 1. The three naturally occurring Trp residues are located at positions 424, 460, and 495. Nine single-Trp mutant peptides were chosen for investigation by time-resolved fluorescence spectroscopy in order to obtain site-specific information on various segments within the channel peptide upon low-pH activation. The specific locales for the single Trp residues within these mutant peptides include Y367W, F404W, F413W, W-424, F431W, F443W,

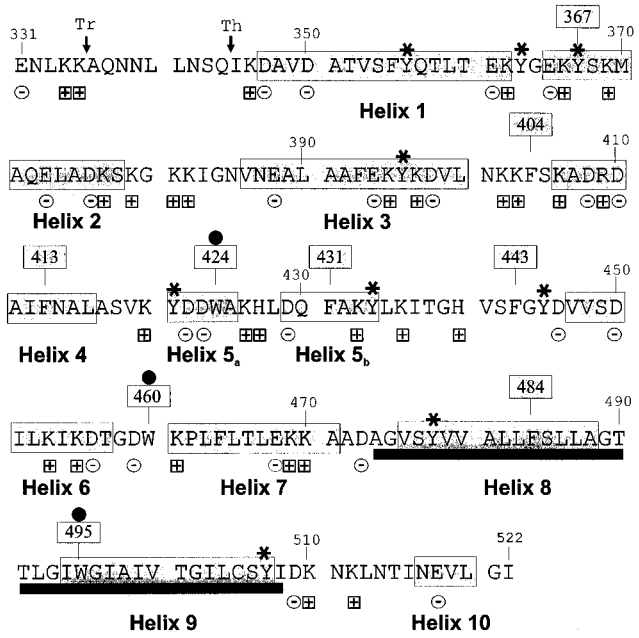

FIGURE 1: Primary sequence of the channel-forming domain of colicin E1 (*18*). The 11 α-helical regions are shown by shading and are according to the recently solved 2.5 Å X-ray structure of colicin E1 (C. Stauffacher, unpublished data). The hydrophobic α-helical hairpin is indicated by the bold line. Charged amino acid residues are indicated and are outlined with a circle or square for negatively and positively charged residues, respectively. The sites where a Trp residue has been substituted into the peptide for either a Phe or a Tyr residue are indicated by numbers bounded by a shaded rectangle. The three naturally occurring Trp residues are indicated with a dot above unshaded rectangles. Tyrosine residues are indicated with an asterisk. The sites of cleavage of the colicin E1 channel peptide by trypsin (Tr) and by thermolysin (Th) are indicated.

W-460, F484W, and W-495. Tyr 367 is located at the N terminus of helix 2 and is largely buried at the interface between helices 8, 9, and 10 in the X-ray structure (*3*). Phe 404 is located in the loop region between helices 3 and 4 and is nearly fully exposed (*13*); Phe 413 is located in the middle of helix 4 and appears to be partially exposed to solvent and relatively close to Trp 495. Trp 424 is largely buried in the middle of helix 5_a, a small polar helix. Phe 431 is located in the middle of small helix 5_b, a very flexible region of the channel peptide, and is mostly buried and inaccessible to the aqueous solvent. Phe 443 is located in the extended loop structure between helices 5_b and 6 and is close enough to residue Lys 470, which is a candidate as a source of the internal quenching seen in the F443W single-Trp mutant (*15*), and the Trp 443 residue is highly exposed to the aqueous solvent (*13*). Trp 460 is located in a moderately polar region within the channel peptide, at the N terminus of helix 7 (C. Stauffacher, unpublished data; Figure 1). Phe 484 is located in the middle of helix 8 and is well sequestered from solvent but may become exposed by any movement of helix 1 or 2. Trp 495 is situated at the N terminus of helix 9 and is only slightly exposed to the aqueous solvent. Furthermore, Trp 484 and 495 are located within the hydrophobic domain of the channel peptide, a nonpolar segment of the peptide consisting of a stretch of 35 amino acid residues; consequently, these latter two Trp residues should report peptide structural changes involving the purported membrane anchor domain.

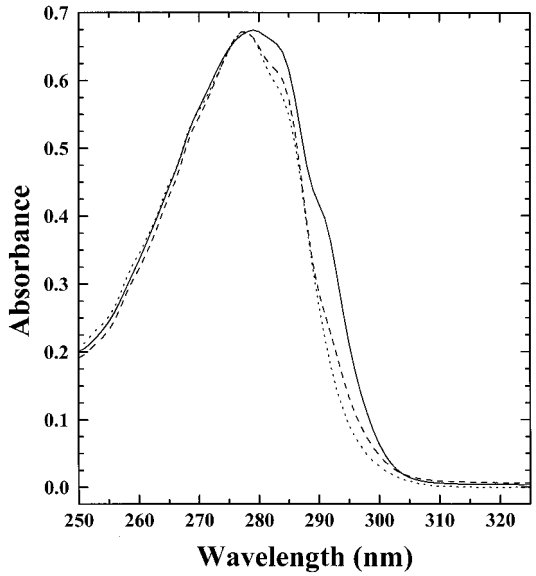

FIGURE 2: Absorption spectra of WT (—), W-424 (– –), and Trp^- (•••) at pH 3.5 in solution. The concentrations of the channel peptides were adjusted so that the absorbance values at 278 nm were identical ($A_{278} = 0.66$) and were at the following concentrations in milligrams per milliliter: WT (0.39), W-424 (0.65), and Trp^- (0.99). The peptides were in 10 mM DMG/100 mM NaCl buffer at pH 3.5 and 20 °C (2 nm band-pass).

Absorption Spectra. The absorption spectra of the WT peptide, the single-Trp-containing channel peptide, W-424, and the peptide devoid of any Trp residue (Trp^-) are shown in Figure 2. The absorption spectra of all the single-Trp mutant peptides were identical to that of W-424. The absorption spectrum of each of the single-Trp mutants had a maximum at 278 nm and, in contrast to that of the wild-type protein, did not exhibit any pronounced shoulder near 292 nm. As expected, the Trp^- peptide showed a significant reduction in its extinction coefficient at 295 nm and hence a significantly higher A_{278}/A_{295} ratio (19.6, cf. 4.9 and 3.4 for W-424 and the WT peptide, respectively). All of the peptides possessed A_{278}/A_{260} ratios between 2.0 and 2.1 indicative of very pure proteins with little, if any, contaminating particulate (scatter-causing) matter and free from nucleic acid contamination. There are nine Tyr residues in the colicin E1 channel domain (Figure 1), and hence, the absorption spectra of the mutants have maxima near 278 nm attributable to the Tyr absorbance and no distinct features which can be attributed to the single Trp residue in the mutants. The shoulder in the absorption spectrum of the wild-type protein is the result of the higher Trp:Tyr ratio in this protein with the Trp spectral features becoming evident.

Fluorescence Spectra and Quantum Yields (Q_F). The fluorescence emission spectra for wild-type colicin and single-Trp peptides for pH values of 3.5 and 6.0 are shown in Figure 3A,C and Figure 3B,D, respectively. These corrected emission spectra have been normalized to the same absorbance at 300 nm and thus represent the relative tryptophan fluorescence quantum yields. The fluorescence maxima (Table 1) varied for the single-Trp peptides depending on the specific location of the Trp residue within the protein structure; the values were similar to those reported earlier (*13*). Notably, the relative quantum yields (Table 1) of the single-Trp peptides exhibited a large range from a low near 0.04 (W-367 at pH 3.5; Figure 3C, Table 1) to a high value of 0.37 (W-495 at pH 6.0; Figure 3B, Table 1).

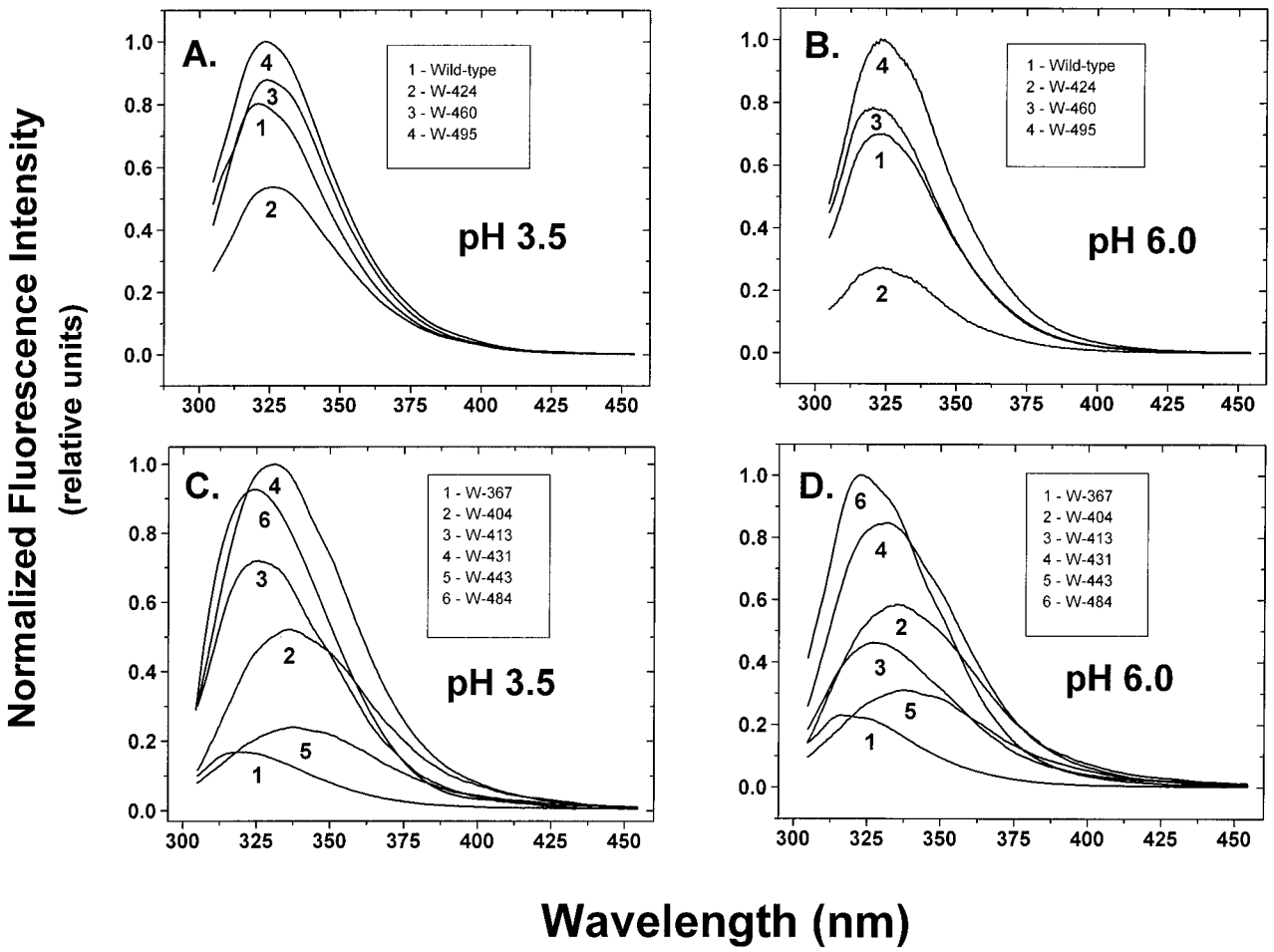

FIGURE 3: Relative fluorescence emission spectra of colicin E1 WT and single-Trp (endogenous) channel peptides (A and B) and exogenous single-Trp mutant channel peptides (C and D) at pH 3.5 (A and C) and at pH 6.0 (B and D). The conditions were as follows: buffer, as in Figure 2; temperature, 20 °C; excitation wavelength, 300 nm; emission wavelength scanned from 305 to 450 nm; and a 4 nm band-pass for both the excitation and the emission. The spectra were corrected for wavelength-dependent bias of the emission optical and detection system. Each spectrum was normalized to the same absorbance at 300 nm ($A_{300\ nm} \cong 0.05$). The various traces are numbered according to the following scheme: (A and B) WT (1), W-424 (2), W-460 (3), and W-495 (4); (C and D) W-367 (1), W-404 (2), W-413 (3), W-431 (4), W-443 (5), and W-484 (6).

At pH 6.0, W-495 has the highest quantum yield followed by W-460, WT and W-484, W-431, W-404 and W-413, W-424, W-443, and W-367. The quantum yield of W-495 is remarkably high, being comparable to the value reported for phosphofructokinase (0.35; *23*). The quantum yield of the wild-type protein was close to the mean value of those of the single-Trp mutants containing a naturally occurring Trp residue, which confirmed the accuracy of the quantum yield measurements.

When the solution pH was changed from 6.0 to 3.5, the quantum yield data shown in Table 1 indicate that W-495 still possesses the highest quantum yield value, followed by W-460, the wild-type and W-431 proteins, W-484, W-413 and W-424, W-404, W-443, and W-367. At this pH, where the peptides are membrane-active, both W-413 and W-424 peptides underwent significant changes (Figure 3A−D, Table 1). Although the fluorescence emission maximum (λ_{em}max) only changed marginally for W-424 (324 to 325 nm), the maximum shifted to a higher energy value for W-413 (332 to 327 nm). More noteworthy, however, was the change in both peptides' respective quantum yields. The quantum yield increased by 80 and 50% for W-424 and W-413, respectively. These significant quantum yield increases are indicative of an altered Trp chemical environment coinciding with a significant pH-induced conformational change in the channel peptide structure near Trp residues 424 and 413. None of the other single-Trp mutant proteins exhibited significant changes in their fluorescence quantum yields except for W-495, which showed a small decrease (14%) upon low-pH activation (Table 1, Figure 3A,B). Also, the fluorescence emission maxima for the majority of the single-Trp mutant peptides showed negligible change with pH with the notable exception being W-413 (Table 1).

The fluorescence spectra of W-460 at both pH values have shoulders near 305 nm which is probably due to a small amount of a Tyr fluorescence component in this peptide even with excitation at 300 nm (Figure 3A,B). A similar case was reported for *subtilisin Carlsberg*, a single-Trp-containing enzyme which has a large number of Tyr residues (*19*). This suggests that some Tyr to Trp energy transfer may occur in the other single-Trp proteins since there was little or no evidence of Tyr fluorescence in the fluorescence emission spectra of the other single-Trp proteins (Figure 3A−D).

Time-Resolved Fluorescence Measurements. In the ensuing discussion, the multiexponential decay behavior which is reported for the various single-Trp mutant proteins is thought to originate from rotamers in the Trp side chain. This interpretation is strongly supported by the work of Dalms *et al.* (*24*), who studied the Trp fluorescence of protein single crystals. Thus, in most cases where double-exponen-

Table 1: Time-Resolved Fluorescence Decay Parameters[a]

peptide	pH	τ_1[b] (ns)	τ_2 (ns)	τ_3 (ns)	C_1[c]	C_2	C_3	λ_1^{max}[d] (nm)	λ_2^{max} (nm)	λ_3^{max} (nm)	λ_{ss}^{max}[e] (nm)	SVR[f]	Q_F[g]	$\langle t \rangle$[h] (ns)	τ_r[i] (ns)
wild-type	3.5	5.05	3.45	0.54	0.21	0.60	0.19	321	325	318	323	1.81	0.25 ± 0.01	3.32	13.3
	6.0	3.98	0.74	−	0.70	0.30	−	324	319	−	323	1.89	0.26 ± 0.01	3.10	11.9
W-367	3.5	3.52	1.45	−	0.76	0.24	−	315	321	−	320	1.67	0.04 ± 0.01	2.68	67.0
	6.0	3.55	1.90	−	0.67	0.33	−	316	320	−	319	1.62	0.06 ± 0.01	2.38	39.7
W-404	3.5	5.90	2.13	0.38	0.22	0.56	0.23	343	331	321	337	1.75	0.13 ± 0.02	1.51	11.6
	6.0	5.60	2.40	0.56	0.27	0.51	0.23	341	329	322	337	1.79	0.15 ± 0.01	1.80	12.0
W-413	3.5	4.39	1.36	0.38	0.43	0.44	0.13	326	326	320	327	1.82	0.18 ± 0.02	2.05	11.4
	6.0	3.73	1.38	0.17	0.32	0.55	0.14	329	326	310	332	1.64	0.12 ± 0.01	1.29	10.8
W-424	3.5	4.56	2.72	0.53	0.43	0.40	0.17	329	322	317	325	1.96	0.18 ± 0.01	3.41	18.9
	6.0	4.65	1.26	0.30	0.23	0.39	0.37	324	321	318	324	1.87	0.10 ± 0.03	1.96	19.6
W-431	3.5	5.78	1.70	−	0.82	0.19	−	331	320	−	334	1.82	0.25 ± 0.01	4.74	19.0
	6.0	5.54	1.64	−	0.80	0.20	−	331	321	−	333	1.85	0.22 ± 0.02	4.43	20.1
W-443	3.5	3.54	1.32	0.28	0.27	0.37	0.37	343	334	325	338	1.59	0.06 ± 0.01	1.06	17.7
	6.0	3.64	1.42	0.27	0.27	0.36	0.37	343	334	320	338	1.65	0.08 ± 0.01	1.12	14.0
W-460	3.5	4.17	1.84	−	0.85	0.15	−	319	309	−	321	1.98	0.27 ± 0.04	4.03	14.9
	6.0	4.41	1.54	−	0.93	0.07	−	316	305	−	323	1.96	0.29 ± 0.04	4.35	15.0
W-484	3.5	4.09	0.82	−	0.88	0.12	−	323	320	−	325	1.69	0.24 ± 0.03	3.60	15.0
	6.0	4.17	1.60	−	0.93	0.07	−	325	315	−	325	1.73	0.26 ± 0.01	3.88	14.9
W-495	3.6	4.66	1.60	−	0.91	0.09	−	326	311	−	324	1.94	0.32 ± 0.01	3.60	10.3
	6.0	4.77	1.47	−	0.93	0.07	−	324	313	−	324	1.98	0.37 ± 0.02	3.88	10.5

[a] The excitation λ was 300 nm with 4 nm slits. Parameters are given for a global fit to 10 data sets collected as a function of emission wavelength (305−400 nm, where the same emission wavelengths were measured for each sample). Stokes Raman scattering at 328 nm was used to determine the instrument response function (FWHM of 60 ps). Data were collected at 80 ps/channel in 2048 channels. The protein concentration in the samples was adjusted so that the A_{300} was between 0.05 and 0.10. The peptides were in 100 mM NaCl/10 mM DMG buffer at the indicated pH. [b] Fluorescence decay times recovered from global analysis. The standard errors, derived from the diagonal elements of the covariance matrix in the nonlinear least-squares analysis, were typically less than 0.01 ns. [c] The emission wavelength-independent fractional concentrations were determined from the relationship $c_i = (A_i/\tau_i)/(\sum A_i/\tau_i)$, where c_i, is the emission wavelength-dependent fractional concentration, A_i is the area of the decay-associated spectrum, and τ_i is the fluorescence decay time of the ith component, respectively (estimated error of ±0.01). [d] Approximate emission maximum of the spectrum associated with a specified decay time component. [e] Steady-state emission maximum (corrected); error of ±1 nm. [f] The reduced χ^2 for the global fit ($\chi^2 = 1$ for an ideal fit) ranged from 1.0 to 1.1 for all samples. The serial variance ratio for the global fit (SVR = 2 for an ideal fit) ranged from 1.59 to 1.98 for global analysis of all samples. [g] The fluorescence quantum yields were measured with λ_{ex} at either 295 or 300 nm with the emission scanned from 305 to 450 nm (excitation and emission slits at 2 and 4 nm, respectively) and NATA (20 °C, $Q_F = 0.14$) as the quantum standard. The temperature was 20 °C. The buffer was 10 mM DMG/100 mM NaCl at pH 3.5 or 6.0; protein concentrations were adjusted so that the absorbance at the excitation wavelength was between 0.05 and 0.10. [h] The mean singlet fluorescence lifetime, $\langle\tau\rangle$, was calculated according to $\langle\tau\rangle = \sum\alpha_i t_i$ where α_i and τ_i are the concentration term and the individual decay time for the ith component calculated from the global, respectively. [i] The calculated (apparent) radiative fluorescence lifetime, τ_r, was determined from the equation $\tau_r = \langle\tau\rangle/Q_F$.

tial decay behavior was observed, the conclusion that follows is that the Trp residue is only able to adopt two rotamer conformations owing to limitations of the volume cavity in its immediate environment. In the case of triple-exponential decay behavior, all three rotamers around the $C_\alpha-C_\beta$ bond can be accommodated in the protein structure. It has been shown (*22*) that the relative proportions of the fluorescence decay components may be correlated with local secondary structure features.

The time-resolved fluorescence decay parameters of the proteins studied in this report are presented in Table 1. The excitation wavelength was set at 300 nm in order to avoid any contribution from Tyr fluorescence and to reduce the significance of Tyr to Trp energy transfer in the data. The parameters are those which were obtained from a global analysis of all of the data sets measured at the different emission wavelengths. All proteins studied showed multi-exponential decay kinetics indicative of the existence of conformational heterogeneity of the Trp residue in the segment of the protein in which it was located (*22*). The fluorescence emission of W-367, W-431, W-460, W-484, and W-495 each had two decay components; the higher τ values were generally characteristic of longer Trp fluorescence lifetimes (3.52−5.78 ns), whereas the second component was usually near 1.5 ns (Table 1). Surprisingly, both fluorescence components from each of the aforementioned peptides were largely indifferent to pH change. It might have been expected that the difference in the decay time parameters for these five peptides would have been greater than those observed since there was a wide range in their quantum yields (0.04−0.37). However, the mean decay times for these peptides, except for W-367, reflect their respective quantum yield values. The calculated (apparent) radiative lifetimes were similar for W-431, W-460, W-484, and W-495 (10.3−20.1 ns), although these values for W-431 and W-495 were higher and lower, respectively, than those for the other two peptides (W-460 and W-484, Table 1). This suggests that the Trp residues are in a similar electronic environment (*25*). Moreover, the Trp residues in these four peptides have been classified as moderately buried on the basis of their accessibility to acrylamide (*13*).

Single-Trp mutant peptide W-367 was clearly different, on the basis of its fluorescence emission properties, than the other four Trp mutant proteins in the aforementioned group. The Trp fluorescence emission of W-367 showed the lowest average lifetime (2.38−2.68 ns), the lowest quantum yield (0.04−0.06), and the highest radiative lifetime values (39.7−67.0 ns). This single-Trp mutant peptide also exhibited the smallest long component lifetime (3.52−3.55 ns) for proteins in this group of colicin channel peptides. Obviously, the Trp residue at position 367 in the peptide sequence is in a chemical environment significantly different from those of any of the other single-Trp peptides that were studied. Tyr 367 (Y367W) is located on the nonpolar face of helix 2 facing inward toward the hydrophobic core of the channel peptide. Furthermore, a careful examination of the colicin E1 channel peptide X-ray structure revealed the proximity of Tyr 367 to the sulfur-containing side chain of Met 370.

Conceivably, replacement of this Tyr residue with Trp would likely result in the interaction between the sulfur atom of Met 370 and the indole side chain of the Y367W mutant. This potential interaction may account for the unusually low quantum yield of W-367 mutant peptide (Table 1) due to the ability of sulfur-containing groups to quench indole fluorescence (*26*). The proximity to a Met side chain may result in one of the three possible Trp rotamers being nonfluorescent due to a static quenching mechanism. The other decay times of the two rotamers would be reduced by the proximity of the Met residue. The apparent difference in the radiative lifetimes of W-367 depending on pH is probably due to the error in measuring such a low quantum yield. In other cases, however, the radiative lifetime differences are significant and important and probably represent the Trp residue located in different electronic environments (*22*, *27*, *28*).

The second group of single-Trp mutants possessed three lifetime decay components and were peptides W-404, W-413, W-424, and W-443 (W-413 and W-424 to be discussed below). W-404 showed considerably higher values than W-443 for all three of its fluorescence decay components (Table 1); both peptides had low average fluorescence lifetime values ($\langle\tau\rangle$, 1.06−1.80 ns). The concentration (C_2) of the τ_2 component was 50% of the total for W-404 with the rest divided equally between the τ_1 and τ_3 decay components (Table 1). In the case of W-443, the C_1 component was lower than the C_2 and C_3 values for their respective τ_1, τ_2, and τ_3 components. However, it is not possible to interpret this behavior in terms of structural features at this time.

The decay time behavior for the WT channel peptide varied with pH. The long decay time component at pH 3.5 (5.05 ns) was slightly higher than that found in the single-Trp (endogenous) channel peptides (Table 1). In contrast, the long decay time value for the WT peptide at pH 6.0 was lower than that for any of the aforementioned single-Trp mutants. Furthermore, the WT showed a change in the number of its decay components with pH (Table 1). This peptide exhibited two components at pH 6.0 and three components at pH 3.5. The magnitude of the shortest lifetime component did not vary with pH. However, its wavelength-independent concentration (C_i) changed from 30 to 19% for pH 6.0 and 3.5, respectively. Conversely, the longest decay time component varied significantly with pH. At pH 6.0, it was 3.98 ns and increased to 5.05 ns upon acidification. Also, an intermediate decay time component (3.45 ns) was present at pH 3.5. The source of these decay time components in the WT peptide is not clear since they do not seem to bear much resemblance to those of the single-Trp (endogenous) mutant channel peptides. However, the pH-sensitive change observed in the WT peptide must originate in a complex fashion from Trp 424 since this Trp was the only residue found in the WT peptide that reported a variation in its decay times with pH. Obviously, the decay times observed for the WT peptide are some weighted average of the individual Trp components.

The fluorescence decay behavior of W-424 and W-413 was strikingly different from that of any of the other single-Trp peptides and underwent a large change with pH. The intermediate decay time of W-424 increased significantly from 1.26 to 2.72 ns upon low-pH activation but did not change for W-413 (1.36 ns, Table 1). In contrast, the longest decay time component for W-413 increased from 3.73 to 4.39 ns upon low-pH activation. This could be rationalized in terms of a major structural change in the protein in the region containing Trp 413 and 424 that is induced by a pH change. The fractional concentrations (Table 1) for W-424 at pH 6.0 are similar to those observed for Trp in an α-helical segment of parathyroid hormone, a small protein with a solvent-exposed Trp residue (*28*). However, Trp 424 is not a solvent-exposed Trp residue (*13*) but is mostly buried within the colicin E1 channel peptide-soluble structure. Therefore, it is presently difficult to assign a given change in the relative concentration parameters of the various decay time components to a specific secondary structural change. Nonetheless, it is clear that there is a significant change in the secondary structure of the channel peptide upon low-pH activation near Trp 424. W-413 likewise shows an increase in the C_1 value with a concomitant decrease in its C_2 value upon low-pH activation of the peptide. However, in contrast to Trp 424, Trp 413 is more exposed to the aqueous solvent than is Trp 424 (*13*), and consequently, it may respond differently to acidification of the aqueous medium.

The decay-associated spectra (DAS) of W-424 and W-413 at pH 3.5 and 6.0 are presented in Figure 4A,B and Figure 4C,D, respectively. These spectra show that at low pH the long (τ_1, 4.56 ns; C_1, 0.43) and the intermediate decay components (τ_2, 2.72 ns; C_2, 0.40) dominate the fluorescence emission of W-424. At pH 6.0, there is a reduction in the relative concentration of the long decay time component (C_1, 0.23) with a concomitant increase in the short decay time component (Table 1, Figure 4A,B). In the case of W-413, the long (τ_1, 4.39 ns; C_1, 0.43) and intermediate decay components (τ_2, 1.36 ns; C_2, 0.44) also dominate the fluorescence emission at low pH. However, at pH 6.0, there is a reduction in the long decay component (C_1, 0.32) with a simultaneous increase in the intermediate decay time component (C_2, 0.55). These observations are consistent with helix 5_a and the N terminus of helix 4 (Figure 1) being relatively unstable secondary structures that possess dynamic characteristics which result in this protein segment (Lys 406−Phe 413) alternating between helices (pH 6.0) and loop-like structures (pH 3.5) that are modulated by solution pH. This phenomenon of chameleon-like behavior of a peptide segment in a protein also was previously observed for the small protein, parathyroid hormone, and the changes in the decay time components of its single Trp residue, going from an α-helix to a random structure upon acidification, correspond to those observed for Trp 424 and 413 (Table 1; *28*).

The DAS of W-431, W-460, W-484, and W-495 were similar and exhibited little change with pH (Table 1, data not shown). For these peptides, there were only two decay time components with the long component dominating the fluorescence emission (C_1 values ranged from 0.80 to 0.93). However, upon low-pH activation, W-460 showed a difference in the fluorescence λ_{em}max values of its two decay time components. In this peptide, both decay time components were more blue-shifted than the corresponding values for all other mutant peptides, except for W-367 (Table 1). The λ_{em}max values for the short decay time of W-460 at pH 6.0 and 3.5 were 305 and 309 nm, respectively, which indicated the presence of a small contribution of Tyr fluorescence (Table 1; C_2, 0.07−0.15). This observation is given further credence by the presence of a shoulder near 305 nm in the steady-state spectra of W-460 (Figure 3A,B). The presence

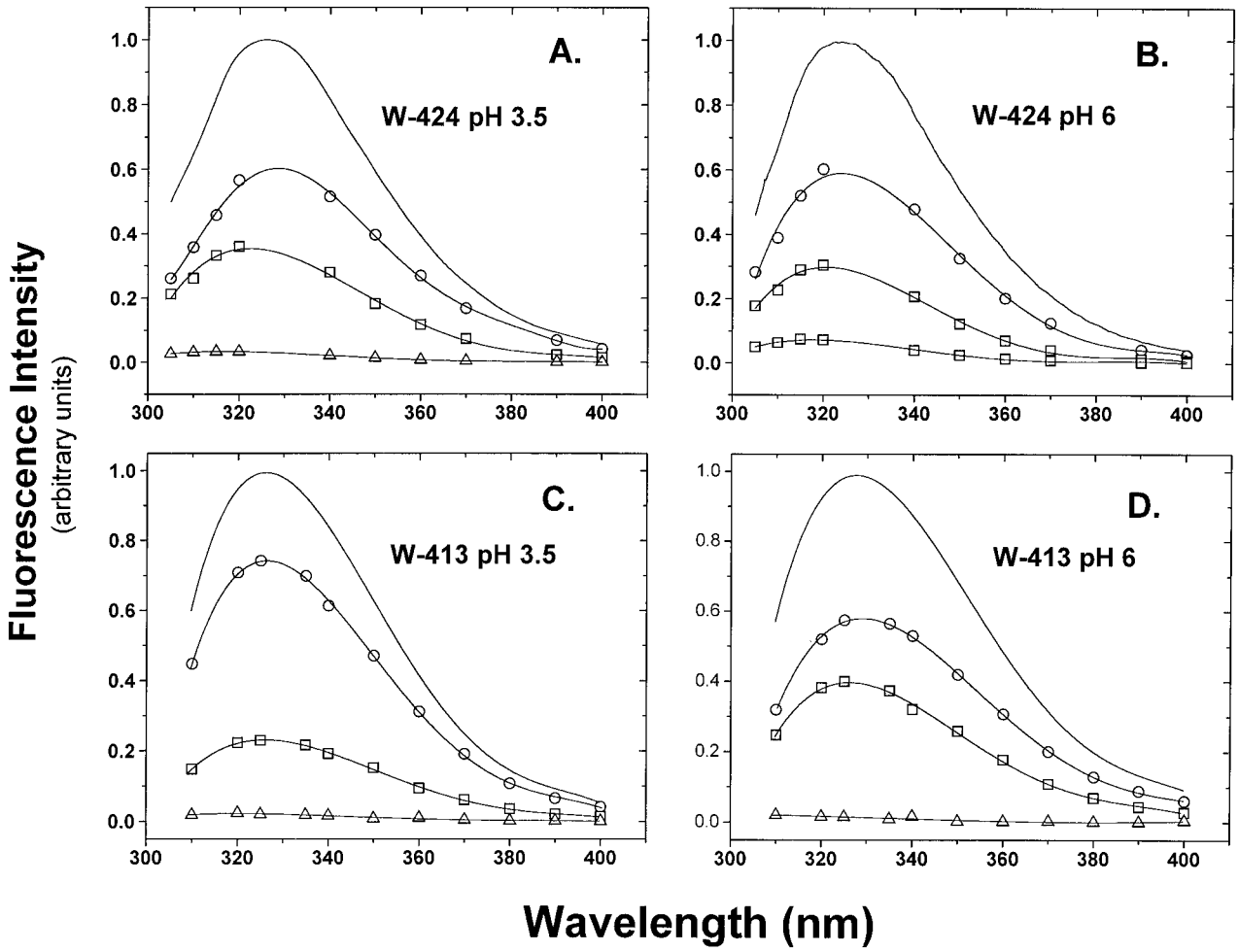

FIGURE 4: Decay-associated emission spectra for W-424 channel peptide at (A) pH 3.5 and (B) pH 6.0 and for W-413 at (C) pH 3.5 and (D) pH 6.0. The buffered solution was identical with that described in Figure 2. Steady-state spectra are indicated by a solid line with no symbols. The circles, squares, and triangles represent (A) the 4.65, 1.26, and 0.30 ns decay time components, (B) the 4.56, 2.72, and 0.53 ns decay time components, (C) the 4.39, 1.36, and 0.38 ns decay time components, and (D) the 3.73, 1.38, and 0.17 ns decay time components, respectively. DAS-propagated errors, computed from the standard errors of the decay time components, are within the contours of the plotted symbols.

of a Tyr component is not evident in any of the other mutant peptides, perhaps because in most cases the Tyr residue(s) responsible for the fluorescence emission in W-460 transfers excited-state energy to this Trp residue. The presence of nine Tyr residues in the channel peptide suggests that the probability of Tyr to Trp energy transfer is high.

The decay time behavior and the DAS of the three Trp residues of the WT protein require comment. All of the decay times of the WT peptide, except for the shortest decay time values at pH 3.5 for WT and W-424, are very different from their respective values in single-Trp mutant peptides containing a naturally occurring Trp residue. For example, it might have been expected that the shorter decay time (0.74 ns) at pH 6.0 (Trp fluorescence for the WT peptide fits a double exponential at pH 6.0) would be close to the average of that same component for the three single-Trp peptides ($\langle\tau\rangle$, 1.42 ns). At pH 3.5, this decay component was 3.45 ns in the WT protein and the largest intermediate decay time value for any of these three mutant peptides was 2.72 ns in W-424. The DAS (data not shown) and the C_i terms also show that the WT fluorescence decay behavior is not a linear combination of the parameters of the three individual mutant proteins. This suggests that there is an interaction between the three Trp residues in the WT protein which leads to more complex decay behavior. A likely possibility is that there is energy transfer between excited states of the Trp 460 and 495 residues owing to their proximity in the protein (~6.5 Å between electronic centers of the two indoles in the X-ray structure). The data clearly show that there is a change in these interactions when the pH is lowered to 3.5, inducing the insertion-competent state (Table 1).

The assignment of the two decay components in each of the W-367, W-431, W-460, W-484, and W-495 single-Trp proteins also requires comment. One possibility might be that the low-intensity component corresponds to a fluorescent protein impurity. However, all evidence was fully consistent with the protein samples being homogeneous single proteins (*13*, *14*, *29*). An alternate explanation is that the 1.5−1.9 ns component represents a small amount of another conformation of the protein or at least of that segment containing the Trp residue or perhaps that it reflects the presence of a small amount of Tyr fluorescence emission. The first possibility may be due to the presence of a small amount of structurally altered (denatured) protein. However, no evidence to support this suggestion is available at the present time. Furthermore, there are other examples where the fluorescence decay behavior of proteins obeys double-exponential decay kinetics (*8*, *9*, *30*). It is reasonable to suggest that, in the interior of the protein these Trp residues which are largely sequestered from the aqueous solvent have

a restricted conformational space and therefore are only able to assume two rotamer populations.

The time-resolved fluorescence data for W-404, W-424, and W-443 suggest that there is more conformational variation in the vicinity of these three Trp residues within the channel peptide and that they are able to take up three different rotamer configurations. The fluorescence data on W-413 and W-424 indicate that the peptide segment containing helices 4 and 5_a show a structural response in concert with low-pH activation. The fluorescence decay behavior of the WT peptide at pH 3.5 suggests that Trp 424 may be the most important emitting species in the WT peptide, since the parameters most clearly resemble those of W-424. This would occur if the orientation or especially the distance between Trp 424 and the other Trp residues was reduced as a result of the pH change. These data corroborate findings from an earlier study where FRET was used to demonstrate that Trp 424 senses conformational changes in the channel peptide upon activation to the insertion-competent state (*14*).

The recent determination of the X-ray structure of the colicin E1 channel peptide (C. Stauffacher, personal communication) at neutral pH provides added insight into the mechanism of low-pH activation of this protein. Careful inspection of this crystal structure provides the impetus for potential explanations of the observed fluorescence data presented in this paper. Upon acidification, both W-424 and W-413 report a proposed transition from helix to coil structure on the basis of the change in the concentrations of the various lifetime components of their respective fluorescence decay profiles. Candidate residues that may respond to a lowered pH environment from 6.0 to 3.5 include Glu, Asp, and perhaps His side chains. Therefore, a likely event associated with the inferred structural change within the channel peptide upon solution acidification may be the destabilization of a salt bridge or critical H-bond involving one of the aforementioned residues in the vicinity of Trp 424 and Trp 413. Inspection of the high-resolution structure of the channel peptide in the vicinity of Trp 424 provides the basis for the following proposal. There are two Asp residues near Trp 424 (Asp 422 and Asp 423), and there is an intrahelical H-bond involving the backbone amino group of Lys 420, at the amino terminus of helix 5_a (Figure 1), and the carboxylate side chain of Asp 423, which serves to stabilize this small helix. A decrease in the solvent pH from 6.0 to 3.5 would be expected to cause a destabilization of this H-bond between the Asp 423 carboxylate oxygen atom and the backbone amino nitrogen of Lys 420 owing to the protonation of the Asp 423 carboxylate group. The weakening of this H-bond may provide the stimulus for the helix-to-coil transition, and it may be this latter transition event that is reported by Trp 424 fluorescence. This helix-to-coil transition, however, does not result in a change in the degree of solvent exposure since the accessibility of Trp 424 to the water-soluble, fluorescence quencher acrylamide does not change significantly with pH (*13*).

Concomitant with the acid-induced helix-to-coil transition is a large increase in the fluorescence quantum yield of W-424 (0.10 to 0.18 for pH 6.0 and 3.5, respectively; Table 1). This enhanced quantum yield of W-424 might implicate greater sequestering from the aqueous solvent upon low-pH activation; however, the aforementioned acrylamide quenching data negate that possibility. One legitimate possibility is that there is a nearby carboxyl group (Asp 446), which is located 4−6 Å distant, which may move further away from the indole ring of Trp 424, resulting in the enhancement in this Trp residue's fluorescence quantum yield. Another possibility is that upon low-pH activation the amide backbone near Trp 424 may move away from this indole side chain with a simultaneous enhancement in its fluorescence quantum yield, since it has recently been shown that the peptide bond quenches indole fluorescence (*31*). Regardless of the specific nature of the conformational rearrangement of this segment of the channel peptide, it is clear that any consideration must comply with an enhancement in the fluorescence quantum yield of Trp 424, implying an increase in the hydrophobicity near this Trp reporter residue or an increase in distance from a nearby quenching moiety, but not to a decreased exposure to the aqueous solvent.

Inspection of the X-ray structure of the channel peptide in the region near Phe 413 (F413W reporter in mutant peptide, W-413) reveals that Trp 413 would be located in the middle of an 11-residue helix, helix 4 (Figure 1). At the N terminus of this helix are located important H-bonds, one between Asp 408 (carboxylate) and the backbone amino group of Ser 405 and another involving a salt link between Asp 410 (carboxylate) and Lys 406 (ammonium) side chains. Protonation of these two Asp residues upon low-pH activation (pH 3.5) would likely result in a destabilization of these two H-bonds and consequently instigate a partial unraveling (a helix-to-coil transition) of the amino-terminal end of helix 4. This idea is given further credence upon consideration of the amino acid residue composition of the N terminus of helix 4, which contains Ser (position 405) and two Asp (positions 408 and 410), which are weak helix-forming residues, implying that the amino end of helix 4 may be structurally unstable upon disruption of the two aforementioned H-bonds. Interestingly, Trp 413 in the F413W mutant peptide (W-413), although situated near the center of helix 4, must sense this helix-to-coil transition occurring at the amino end of this helix. However, it is difficult to speculate as to the origin of the increase in the fluorescence quantum yield of W-413 since the X-ray structure is for the wild-type peptide (Phe 413). However, in contrast with those for Trp 424, fluorescence data from previous work (*13*) indicated that upon low-pH activation, Trp 413 becomes more buried and reports a blue shift (5 nm) in its λ_{em}max which corroborates the observed increase in its fluorescence quantum yield (0.12 to 0.18 for pH 6.0 and 3.5, respectively; Table 1).

The anisotropy decay profiles for W-424 and the WT channel peptides at pH 3.5 are shown in Figure 5A,B, respectively. The anisotropy decay data for both W-460 and W-495 were nearly identical with the data shown in Figure 5A. The anisotropy decay values were similar for each of the three mutants and did not change significantly with pH and hence the activation state of the channel peptides. However, the anisotropy decay curves for the WT channel peptide were different from those of the single-Trp mutant peptides ($\theta_1 = 7.4$ ns and $r_o = 0.10$ and $\theta_2 = 0.28$ ns and $r_o = 0.11$ for the slow and fast components of the WT peptide, respectively, as compared with $\theta = 12.8$ ns, and $r_o = 0.22$ for W-424; both peptides at pH 3.5). It is of interest to note that an r_o value near 0.3 is often found when applying the phase/modulation analyses of anisotropy decay and that the values obtained herein by the photon counting method are considerably smaller than 0.3; however, fixing such large

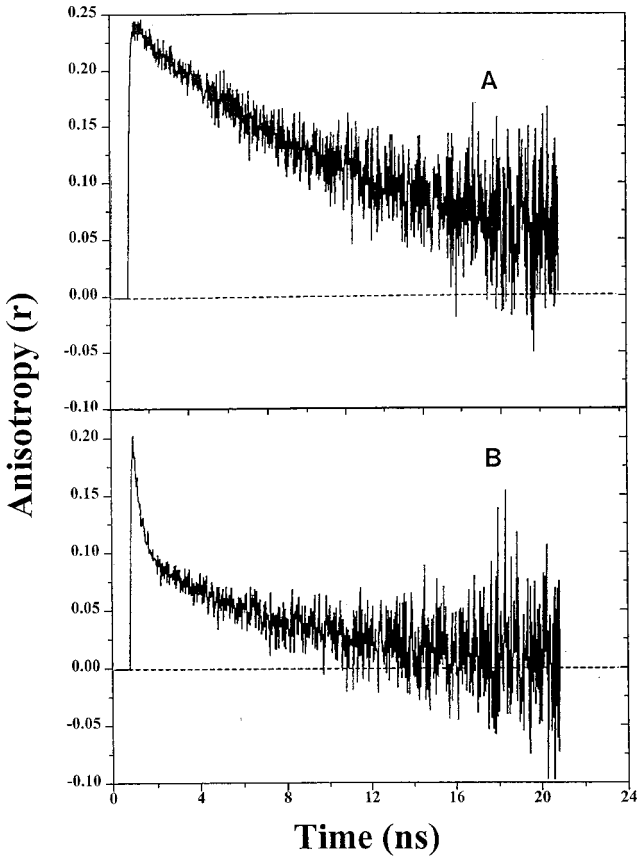

FIGURE 5: Fluorescence anisotropy decay profiles for colicin E1 channel peptides at pH 3.5: (A) W-424 and (B) WT. These are the fluorescence anisotropy decay curves constructed from the individual parallel and perpendicular components (see Materials and Methods). The anisotropy decay parameters were obtained by a linked convolution analysis of the parallel and perpendicular decay profiles. Experimental conditions were as described in Figure 2 and Table 1.

r_o values may distort the recovery of the real θ value (*32*). It is clearly evident that the slope of the time-resolved anisotropy decay profile for the WT peptide is steeper than the corresponding profile for the W-424 mutant (Figure 5). The WT peptide possessed a shorter-lived component that was not present in any of the single-Trp mutant peptides, possibly attributable to FRET. This postulate could be tested by preparing a complement of mutant peptides possessing pairs of Trp residues, i.e., W-424 and W-460, W-424 and W-495, etc. However, careful examination of the X-ray structure of the channel peptide indicated that Trp 460 and 495 are sufficiently close in space for FRET to occur between them (6.5 Å), whereas Trp 424 is much farther away from both of the other two endogenous Trp residues (~16 and 17.5 Å from Trp 460 and 495, respectively).

The anisotropy decay behavior of the WT peptide may be attributed to a rapid depolarization of the fluorescence as a result of energy transfer between the Trp residues. The rotational correlation times for each of the Trp mutants were higher than those expected for the whole peptide on the basis of calculations using the relationship $\theta = \eta V/RT$, where η is the viscosity in poise, V is the molar volume of the rotating object, R is the gas constant, and T is the temperature (kelvin). The calculated value for θ is 7.5 ns in aqueous medium at 20 °C for a globular protein with a molecular weight of approximately 19 700 Da. The experimentally determined value of θ (12.8 ns) for W-424 (similar to the values for the other two Trp mutants at both pH values) was higher than the calculated value (θ = 7.5 ns). However, the error associated with the fluorescence measurement of θ may be quite large considering that the anisotropy decay curves terminate at 20 ns, before the plateau value has been reached, due to the weak fluorescence signal beyond 20 ns (Figure 5). Given the fact that the measured θ value for the single-Trp mutants was higher (12.8 ns, slower motion) than the calculated value rather than lower (7.5 ns, faster motion), this indicated that each of the three naturally occurring tryptophans in the colicin E1 channel peptide are in very rigid environments in the solution structure of the protein and these residues exhibit only a limited amount of flexibility (on the nanosecond time scale). Also, activation of the channel peptide to its insertion-competent state does not affect the mobility of the Trp residues which is in agreement with previous results (*6*, *14*) that indicate that activation does not involve a large structural change within the channel peptide.

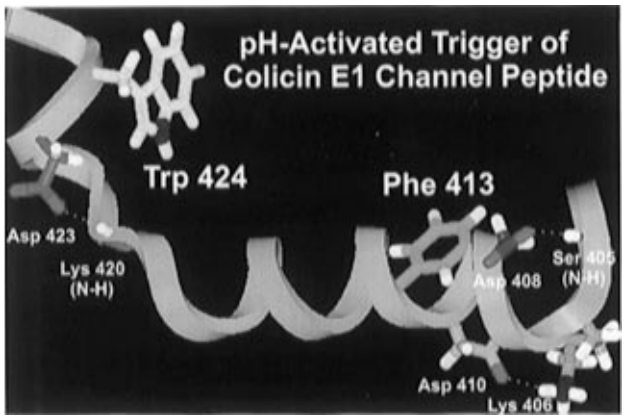

FIGURE 6: Ribbon topology diagram of the proposed pH trigger of the colicin E1 channel peptide. The drawing was prepared using BIOSYM Insight II software and is based on the data for the X-ray structure of the thermolytic peptide of colicin E1 (C. Stauffacher, unpublished). The peptide backbone is shown in ribbon format (cyan), and the side chains of Trp 424 (yellow), Asp 423 (magenta), Phe 413 (emerald green), Asp 410 (orange), Asp 408 (purple), and Lys 406 (salmon pink) are shown in stick format. The NH backbone atoms are also shown in stick format for Lys 420 and Ser 405. The residues displayed in stick format distinguish the nitrogen (blue), oxygen (red), and hydrogen (white) atoms in unique colors. The pH-sensitive H-bonds between donor and acceptor atoms are shown by dashed white lines.

The fluorescence data generated during the course of this study from nine single-Trp mutant and WT peptides, combined with the recent X-ray structural data of the colicin E1 thermolytic channel peptide, provide compelling evidence for the existence within this peptide structure of a pH-activated trigger mechanism required as a prerequisite for membrane bilayer interaction. This trigger finds its operational center at helix 5_a and at the N terminus of helix 4 (Figure 6). The trigger is actuated by protonation of three Asp residues leading to the destabilization of one salt bridge, Lys 406−Asp 410, and two H-bond links, Ser 405−Asp 408, and Lys 420−Asp 422. The disruption of one or all of these H-bond links may provide the driving force for a cascade of structural events within the channel peptide that is reported by Trp 413 and 424. It is tempting to speculate that this pH-induced conformational change within the channel peptide serves to activate the peptide from the soluble, membrane insertion-incompetent state to the membrane insertion-competent state that is

capable of bilayer association and, in the presence of a membrane potential, channel formation.

Previously, Shiver *et al.* (*33*) investigated the role of Glu 468, a conserved acidic residue among the family of channel-forming colicins, in the acidic pH requirement for colicin E1 *in vitro* channel activity. Mutations of this conserved Glu residue were made to amino acids Ser, Gln, Lys, and Leu. All of the mutant colicins possessed high *in vivo* cytotoxic activity, but their *in vitro* channel activities were lower than that for for the WT protein. However, the residual pH dependence for channel activity indicated that more than one carboxylic acid residue must be protonated to account for the increased activity at acidic pH values. Nonetheless, a role for Glu 468 in the mechanism of channel formation or function was implied from the results of this study. It is certainly of interest to note that including Glu 468 there are six acidic residues conserved in aligned sequences of the channel-forming colicins (E1, Ia, Ib, A, B′, and N; *33*, *34*). Furthermore, it is noteworthy to consider that both Asp 408 and Asp 423 (except for colicin Ib) are among this group of conserved acid residues within the channel-forming colicin family. Additionally, Asp 410 is a conserved acidic residue for four of the six channel-forming colicins (*34*). Obviously, the conserved nature of these acidic residues, proposed as part of the intricate mechanism of the pH-activated trigger of colicin E1, adds credence to their potential importance for colicin channel function.

Presently, in progress are experiments designed to test this hypothesis by substituting the H-bond acceptor residues, Asp 410, 408, and 423, with other residues incapable of H-bond formation in order to prevent H-bond and/or salt bridge formation and to observe the effect these amino acid substitutions have on the pH-dependent activation of the channel peptide.

ACKNOWLEDGMENT

We thank Don Krajcarski of the Institute for Biological Sciences (National Research Council, Ottawa, Canada) for technical assistance. We are indebted to Patricia Elkins for kindly providing the X-ray coordinates for the colicin E1 thermolytic channel peptide prior to their publication. We also thank Cyndy Stauffacher for many helpful and insightful discussions concerning the X-ray structure of the channel peptide. Furthermore, we gratefully acknowledge the contribution of Bill Cramer regarding the initiation of this project.

REFERENCES

1. Kagan, B. L., Finkelstein, A., and Columbini, M. (1981) *Proc. Natl. Acad. Sci. U.S.A. 78*, 4950−4954.
2. Farahbakhsh, Z. T., and Wisnieski, B. J. (1989) *Biochemistry 28*, 580−585.
3. Cramer, W. A., Heymann, J. B., Schendel, S. L., Deriy, B. N., Cohen, F. S., Elkins, P. A., and Stauffacher, C. V. (1995) *Annu. Rev. Biomol. Struct. 24*, 611−641.
4. Lakey, J. H., van der Goot, F. G., and Pattus, F. (1994) *Toxicology 87*, 85−108.
5. Merrill, A. R., Cohen, F. S., and Cramer, W. A. (1990) *Biochemistry 29*, 5829−5836.
6. Schendel, S. L., and Cramer, W. A. (1994) *Protein Sci. 3*, 2272−2279.
7. Hutnik, C. M. L., MacManus, J. P., Banville, D., and Szabo, A. G. (1990) *J. Biol. Chem. 265*, 11456−11464.
8. Royer, C. (1992) *Biophys. J. 63*, 741−750.
9. Kim, S.-J., Chowdhury, F. N., Stryjewski, W., Younathan, E. S., Russo, P. S., and Barkley, M. D. (1993) *Biophys. J. 65*, 215−226.
10. Hasselbacher, C. A., Rusinova, E., Waxman, E., Rusinova, R., Kohanski, R. A., Lam, W., Guha, A., Du, J., Lin, T. C., Polikarpov, I., Boys, C. W. G., Nemerson, Y., Konigsberg, W. H., and Ross, J. B. A. (1995) *Biophys. J. 69*, 20−29.
11. Pokalski, C., Wick, P., Harms, E., Lytle, F. E., and Van Etten, R. L. (1995) *J. Biol. Chem. 270*, 3809−3815.
12. Merrill, A. R., and Cramer, W. A. (1990) *Biochemistry 29*, 8529−8534.
13. Merrill, A. R., Palmer, L. R., and Szabo, A. G. (1993) *Biochemistry 32*, 6974−6981.
14. Steer, B. A., and Merrill, A. R. (1994) *Biochemistry 33*, 1108−1115.
15. Steer, B. A., and Merrill, A. R. (1995) *Biochemistry 34*, 7225−7233.
16. Cleveland, M. B., Slatin, S., Finkelstein, A., and Levinthal, C. (1983) *Proc. Natl. Acad. Sci. U.S.A. 80*, 8706−3710.
17. Laemmli, U. K. (1970) *Nature 227*, 680−685.
18. Yamada, M., Ebina, Y., Mayato, T., Nakazawa, T., and Nakazawa, A. (1982) *Proc. Natl. Acad. Sci. U.S.A. 79*, 2827−2831.
19. Willis, K. J., and Szabo, A. G. (1989) *Biochemistry 28*, 4902−4908.
20. Zuker, M., Szabo, A. G., Bramall, L., Krajcarski, D. T., and Selinger, B. (1985) *Rev. Sci. Instrum. 56*, 14−22.
21. Knutson, J. R., Beechem, J. M., and Brand, L. (1983) *Chem. Phys. Lett. 102*, 501−507.
22. Willis, K. J., Neugebauer, W., Sikorska, M., and Szabo, A. G. (1994) *Biophys. J. 66*, 1623−1630.
23. Eftink, M. R. (1991) *Methods of Biochemical Analysis Volume 35: Protein Structure Determination* (Suelter, C. H., Ed.) pp 127−205, John Wiley, New York.
24. Dahms, T. E., and Szabo, A. G. (1995) *Biophys. J. 69*, 569−576.
25. Szabo, A. G., and Fierman, C. (1992) Time-Resolved Laser Spectroscopy in Biochemistry III, *Proc. SPIE-Int. Soc. Opt. Eng., 1640*, 70−80.
26. Permyakov, E. A. (1993) in *Luminescent Spectroscopy of Proteins*, CRC Press, Boca Raton, FL.
27. Schauerte, J. A., and Gafni, A. (1989) *Biochemistry 28*, 3948−3954.
28. Willis, K. J., and Szabo, A. G. (1992) *Biochemistry 31*, 8924−8931.
29. Palmer, L. R., and Merrill, A. R. (1994) *J. Biol. Chem. 269*, 4187−4193.
30. Hutnik, C. M. L., and Szabo, A. G. (1989) *Biochemistry 28*, 3935−3939.
31. Chen, Y., Liu, B., Yu, H.-T., and Barkley, M. D. (1996) *J. Am. Chem. Soc. 118*, 9271−9278.
32. Hamman, B. D., Oleinokov, A. V., Jokhadze, G. G., Traut, R. R., and Jameson, D. M. (1996) *Biochemistry 35*, 16672−16679.
33. 33. Shiver, J. W., Cramer, W. A., Cohen, F. S., Bishop, L. J., and de Jong, P. J. (1987) *J. Biol. Chem. 262*, 14273−14281.
34. Cramer, W. A., Cohen, F. S., Merrill, A. R., and Song, H. Y. (1990) *Mol. Microbiol. 4*, 519−526.

BI970222I